Understanding the Selectivity in Hydrogenation of α,β-Unsaturated Aldehydes: A Water-Assisted Mechanism

Jérôme Joubert and Françoise Delbecq*

Laboratoire de Chimie-UMR CNRS 5182, Ecole normale supérieure de Lyon, 46 allée d'Italie, 69364 Lyon Cedex 07, France

Received September 9, 2005

The mechanisms of the competitive C═C and C═O hydrogenations of the α,β-unsaturated aldehydes by $[RuH_2(PH_3)_3]$ are investigated by means of calculations based on density functional theory. The classical mechanism via double-bond insertion into the Ru−H bond followed by σ-bond metathesis does not explain the selectivity to the unsaturated alcohol, since the C═C hydrogenation is found to be easier than the C═O hydrogenation, both thermodynamically and kinetically. A new water-assisted mechanism is presented in which the C═O hydrogenation is clearly favored. This allows us to explain the preferred formation of the unsaturated alcohol, particularly true in biphasic media.

1. Introduction

The synthesis of unsaturated alcohols by hydrogenation of α,β-unsaturated aldehydes is employed in the field of fragrance and flavor chemistry.[1] Hydrogenation selectivity toward one or the other double bond (see Scheme 1) is the challenging part of this synthesis, which can be performed by selective catalytic processes.

Homogeneous catalysis is used in 15% of industrial selective hydrogenations of α,β-unsaturated aldehydes.[2] Although the use of ruthenium complexes for such a purpose is well documented from an experimental point of view, no clear explanation of the hydrogenation selectivity has been proposed for these catalysts, which behave quite differently from cobalt complexes for which mechanistic investigations have been performed.[3]

Following the hypothesis that the hydrogenation of α,β-unsaturated aldehydes occurs via the activation of a double bond by coordination on a metallic fragment, we proposed a study of the relative stability of coordinated α,β-unsaturated aldehydes on ruthenium complexes.[4] The higher stability of the η^2(C,C) coordination mode[4] cannot justify the selective hydrogenation of the C═O bond obtained with such catalysts.

In this work, our aim was to study the mechanism of C═O and C═C hydrogenations and particularly to explain the selectivity toward C═O hydrogenation in biphasic media. We have performed Gibbs free energy calculations along the hydrogenation mechanisms, which can be called classical mechanisms, considering a succession of elementary steps. Then, we have considered a solvent-assisted mechanism. In fact, although some homogeneous hydrogenations are performed in organic solvent which cannot have any specific interaction with the complexes involved in the catalytic cycles,[5] many of them take place in biphasic aqueous/organic media, in which water can have an influence on the reactivity by its coordination on the ruthenium complexes or on the substrate. In such media, different substrates[6] have been studied as well as different catalysts.[7] The kinetics is influenced by pressure, catalyst concentration, and phosphine concentration.[8] The selectivity toward C═O hydrogenation is affected by the hydrogen pressure[9] and the pH.[10]

Scheme 1. Competitive Hydrogenation of α,β-Unsaturated Aldehydes

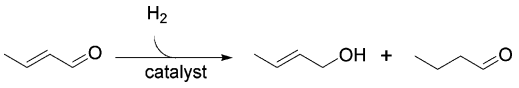

We used crotonaldehyde as a typical α,β-unsaturated aldehyde for this study, as it is used experimentally and leads to a good selectivity toward C═O hydrogenation. In agreement with experimental studies, we consider $[RuH_2(PR_3)_3]$ as the catalytic complex which leads to preferential C═O hydrogenation. This complex is obtained by the dissociation of a phosphine from $[RuH_2(PR_3)_4]$ which is involved in the equilibrium presented in Scheme 2. It has been proved that $[RuH_2(PR_3)_4]$ is the predominant complex in a basic medium with an excess of phosphine, this type of medium being the kind that favors C═O hydrogenation.[10]

Scheme 2. Equilibrium between Ru Catalyst Precursors

$$HCl + RuH_2(PR_3)_4 \rightleftarrows H_2 + PR_3 + RuClH(PR_3)_3$$

2. Computational Details

The calculations have been performed with the Gaussian03[11] code at the DFT/B3LYP level.[12,13] Hay and Wadt effective core potentials have been used for Ru and P with the LANL2DZ basis set.[14] Polarization orbitals have been added to phosphorus atoms. Carbon,

* To whom correspondence should be addressed. E-mail: francoise.delbecq@ens-lyon.fr.

(1) (a) Bauer, K.; Garbe, D. *Common Fragrance and Flavour Materials*; VCH: New York, 1985. (b) Bauer, K.; Garbe, D. *Ullman Encyclopedia*, 3rd ed.; VCH: New York, 1988, Vol. A11.

(2) Keim, W. *Angev. Chem., Int. Ed. Engl.* **1990**, *29*, 235.

(3) Huo, C. F.; Li, Y. W.; Beller, M.; Jiao, H. *Organometallics* **2004**, *23*, 2168.

(4) Joubert, J.; Delbecq, F. *J. Organomet. Chem.* **2006**, in press.

(5) (a) Sanchez-Delgado, R. A.; Andriollo, A.; Valencia, N. *J. Mol. Catal.* **1984**, *24*, 217. (b) Sanchez-Delgado, R. A.; De Ochoa, O. L. *J. Mol. Catal.* **1979**, *6*, 303. (c) Brouckova, Z.; Czakova, M.; Capka, M. *J. Mol. Catal.* **1985**, *30*, 241.

(6) Nomura, K. *J. Mol. Catal. A: Chem.* **1998**, *130*, 1.

(7) Hernandez, M.; Kalck, P. *J. Mol. Catal. A: Chem.* **1997**, *116*, 131.

(8) (a) Darensburg, D.; Joo, F.; Kannisto, M.; Katho, A.; Reibenspies, J.; Daigle, D. *Inorg. Chem.* **1994**, *33*, 200. (b) Grosselin, J. M.; Mercier, C.; Allmang, G.; Grass, F. *Organometallics* **1991**, *10*, 2126.

(9) Papp, G.; Elek, J.; Nadasdi, L.; Laurenczy, G.; Joo, F. *Adv. Synth. Catal.* **2003**, *345*, 172.

(10) (a) Joo, F. *Acc. Chem. Res.* **2002**, *35*, 738. (b) Papp, G.; Kovacs, J.; Benyei, A.; Laurenczy, Y.; Nadasdi, L.; Joo, F. *Can. J. Chem*, **2001**, *79*, 635. (c) Joo, F.; Kovacs, J.; Benyei, A.; Katho, A. *Catal. Today* **1998**, *42*, 441.

10.1021/om050782a CCC: $33.50
Publication on Web 01/21/2006

oxygen, and hydrogen atoms have been treated with the D95(d,p) Dunning basis set.[15] Some tests with the triple-ζ basis set 6-311G,[16] the SDD effective core potentials,[17] and the BPW91 functional[12,18] have not shown any significant changes. The phosphine ligands have been simplified for mechanism investigations, PPh_3 being replaced by PH_3.

All intermediates and transition states have been optimized, and frequency analyses have been performed to be sure that no imaginary frequency occurs for intermediates and that only one occurs for transition states. Gibbs free energies of reaction and activation Gibbs free energies have been calculated for gas-phase reaction using the values given by the codes for $T = 298$ K and $P = 1$ atm.

The basis set superposition errors for bimolecular reactions have been evaluated to be less than 3.5 kJ mol^{-1} and have not been taken into account in results we present here.

3. Classical Mechanisms

Several mechanisms have been proposed for the hydrogenation of ketones by ruthenium complexes (for a review, see ref 19). One of them consists of the coordination of the reactant after departure of a phosphine followed by hydride migration. For the hydrogenation of C═C bonds also, the coordination of the olefin is a primary step of the reaction.[20] Hence, we will focus now on the hydrogenation mechanisms of crotonaldehyde via hydride cis migration to a coordinated π system (or double-bond insertion into the ruthenium−hydride bond). This elementary step can be followed by two types of product elimination: reductive elimination or σ-bond metathesis with dihydrogen (see Scheme 3). Both will be investigated for C═O and C═C hydrogenation.

The complete study of the coordination modes has been reported elsewhere.[4] We will expose in detail the hydrogenation reactions which involve the most stable intermediates **1** and **2** (see Figure 1) where the phosphines are in a meridian position, as they are the most stable isomers. Hydrogenation via similar pathways starting from other isomers (**3**−**5**; see Figure 1) has also been studied, which does not affect the conclusions. Isomers **3**−**5** are the most stable complexes on the metallic fragment, with a facial position of phosphines.

Scheme 3. Classical Hydrogenation Mechanisms: (a) C═O; (b) C═C

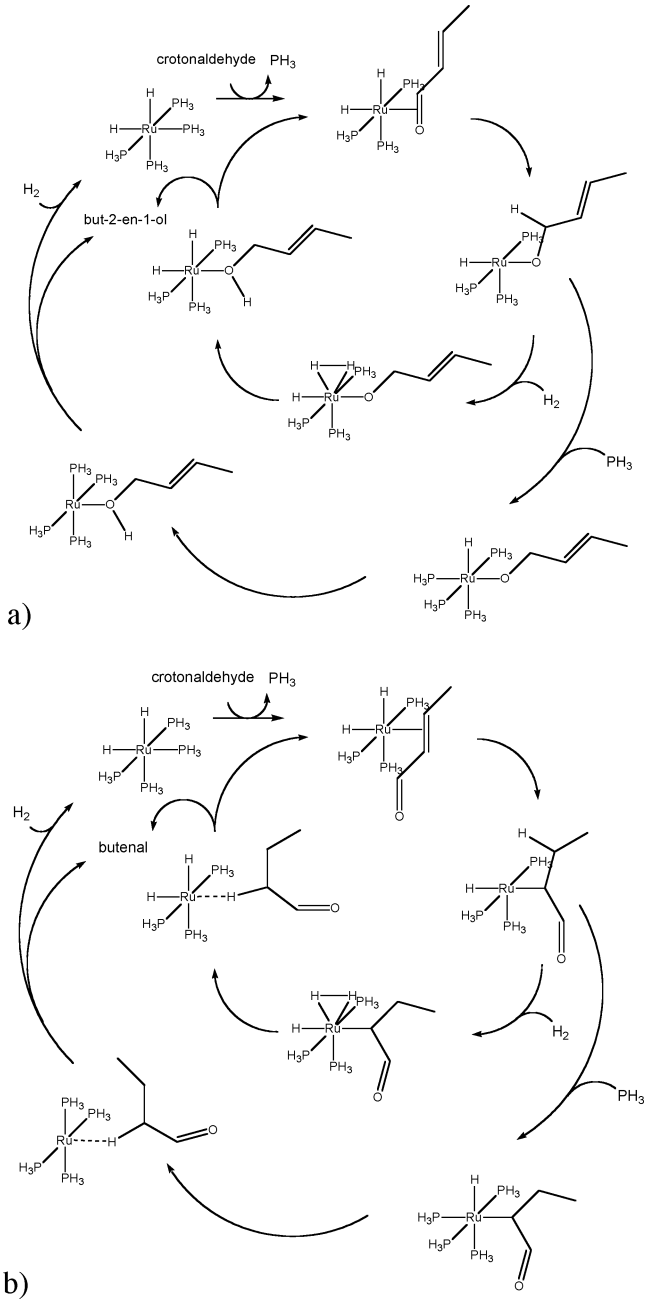

3.1. Cis Migration. Four sites of crotonaldehyde can be involved in the cis migration of the hydride: the four atoms of the π system. The cis migration on the oxygen atom is not possible in the different isomers, due to geometrical considerations: the oxygen atom is never near the hydride. **6** and **7**, the products of cis migration from **1** and **2**, respectively, are represented in Figure 2. They both have an agostic bond to saturate the complexes, which have only 16 electrons without this interaction. In **6**, the Ru−H bond is 1.77 Å, the C−H bond is 1.34 Å, and the Ru−O−C angle is 80.6°. In **7**, the Ru−H bond is 1.88 Å, the C−H bond is 1.22 Å, and the Ru−C−C

(11) Frisch, M. J.; Trucks, G. W.; Schlegel, H. B.; Scuseria, G. E.; Robb, M. A.; Cheeseman, J. R.; Montgomery, J. A., Jr.; Vreven, T.; Kudin, K. N.; Burant, J. C.; Millam, J. M.; Iyengar, S. S.; Tomasi, J.; Barone, V.; Mennucci, B.; Cossi, M.; Scalmani, G.; Rega, N.; Petersson, G. A.; Nakatsuji, H.; Hada, M.; Ehara, M.; Toyota, K.; Fukuda, R.; Hasegawa, J.; Ishida, M.; Nakajima, T.; Honda, Y.; Kitao, O.; Nakai, H.; Klene, M.; Li, X.; Knox, J. E.; Hratchian, H. P.; Cross, J. B.; Bakken, V.; Adamo, C.; Jaramillo, J.; Gomperts, R.; Stratmann, R. E.; Yazyev, O.; Austin, A. J.; Cammi, R.; Pomelli, C.; Ochterski, J. W.; Ayala, P. Y.; Morokuma, K.; Voth, G. A.; Salvador, P.; Dannenberg, J. J.; Zakrzewski, V. G.; Dapprich, S.; Daniels, A. D.; Strain, M. C.; Farkas, O.; Malick, D. K.; Rabuck, A. D.; Raghavachari, K.; Foresman, J. B.; Ortiz, J. V.; Cui, Q.; Baboul, A. G.; Clifford, S.; Cioslowski, J.; Stefanov, B. B.; Liu, G.; Liashenko, A.; Piskorz, P.; Komaromi, I.; Martin, R. L.; Fox, D. J.; Keith, T.; Al-Laham, M. A.; Peng, C. Y.; Nanayakkara, A.; Challacombe, M.; Gill, P. M. W.; Johnson, B.; Chen, W.; Wong, M. W.; Gonzalez, C.; Pople, J. A. *Gaussian 03*, revision C.02; Gaussian, Inc.: Wallingford, CT, 2004.

(12) (a) Becke, A. D. *Phys. Rev. A* **1988**, *38*, 3098. (b) Becke, A. D. *J. Chem. Phys.* **1993**, *98*, 1372. (c) Becke, A. D. *J. Chem. Phys.* **1993**, *98*, 5648.

(13) Lee, C.; Yang, W.; Parr, R. G. *Phys. Rev. B* **1988**, *37*, 785.

(14) (a) Hay, P. J.; Wadt, W. R. *J. Chem. Phys.* **1985**, *82*, 299. (b) Wadt, W. R.; Hay, P. J. *J. Chem. Phys.* **1985**, *82*, 284. (c) Hay, P. J.; Wadt, W. R. *J. Chem. Phys.* **1985**, *82*, 270.

(15) Dunning, T. H.; Hay, P. J. In *Modern Theoretical Chemistry*; Schaefer, H. F., III, Ed.; Plenum: New York, 1976; Vol. 3, pp 1−28.

(16) (a) McLean, A. D.; Chandler, G. S. *J. Chem. Phys.* **1980**, *72*, 5639. (b) Krishnan, R.; Binkley, J. S.; Seeger, R.; Pople, J. A. *J. Chem. Phys.* **1980**, *72*, 650.

(17) Fuentealba, P.; Preuss, H.; Stoll, H.; Szentpaly, L. V. *Chem. Phys. Lett.* **1989**, *89*, 418.

(18) Burke, K.; Perdew, J. P.; Wang, Y. In *Electronic Density Functional Theory: Recent Progress and New Directions*; Dobson, J. F., Vignale, G., Das, M. P., Eds.; Plenum: New York, 1998.

(19) Clapham, S. E.; Hadzovic, A.; Morris, R. H. *Coord. Chem. Rev.* **2004**, *248*, 2201.

(20) Martin, P.; McManus, N. T.; Rempel, G. L. *J. Mol. Catal. A: Chem.* **1997**, *126*, 115.

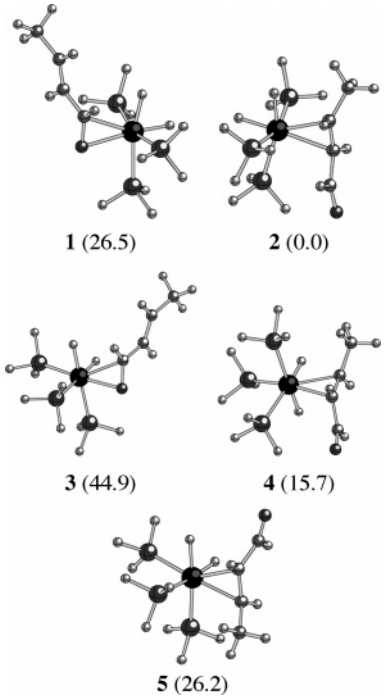

Figure 1. Starting complexes for hydrogenation with, in parentheses, their relative Gibbs free energies in kJ mol^{-1}.

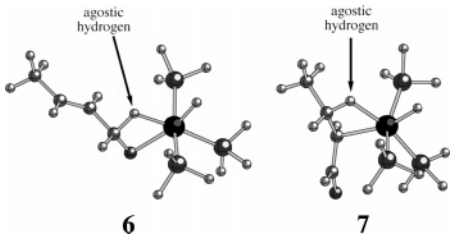

Figure 2. Products of cis migration starting from complexes **1** and **2**.

Table 1. Energetic Data (in kJ mol^{-1}) for the Classical Mechanisms

reactant	product	ΔE	ΔG	$\Delta E^{\ddagger}$	$\Delta G^{\ddagger}$
		Cis Migration			
1	**6**	47	54	50	51
2	**7**	33	35	43	39
		Coordination of H_2			
6	**10**	−43	8	7	52
7	**11**	−48	8	7	52
		σ-Bond Metathesis			
10	**12**	−85	−76	19	25
11	**13**	−61	−66	20	16

angle is 78.4°. Nonrepresented structures of the products from cis migration on **3**−**5** have similar properties. The energetic data for these cis migrations are reported in Table 1.

Notice that the reactions are strongly endothermic. For the reaction **1** → **6**, we can observe that, even if the barrier exists when speaking about internal energy, it disappears when speaking about Gibbs free energy. This would mean that the reaction is not activated (or very little activated): the barrier to be passed over is approximately the thermodynamic difference between products and reactants.

The difference between the two barriers can be explained by orbital analysis. The LUMOs of **1** and **2** are shown in Figure 3. The LUMO is more developed on the carbon C3 in complex **2** than it is on the carbon C1 in **1**: the electrophilicity of **2** is

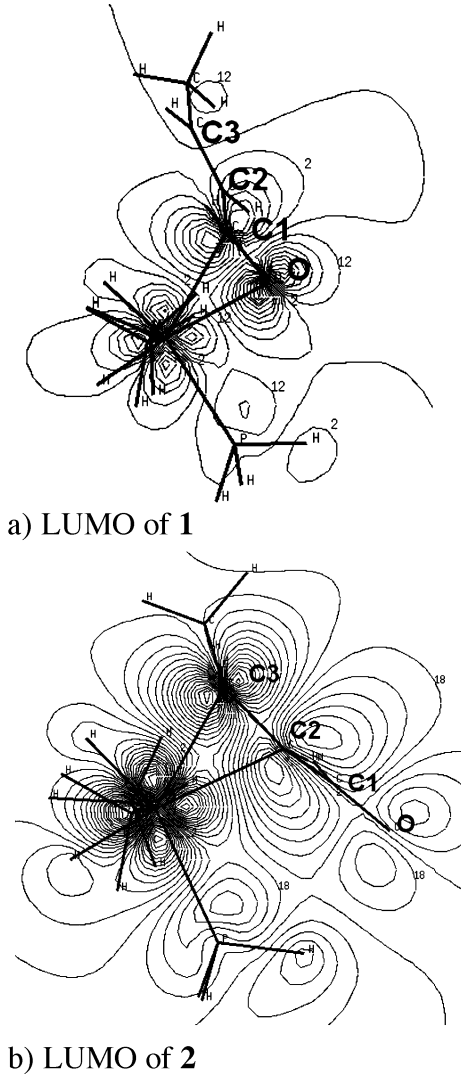

Figure 3. LUMO isodensity curves of starting complexes **1** and **2** in the plane of Ru, hydride, and carbon involved in the cis migration.

higher than that of **1**. As a result, the activation barrier for the cis migration is higher for **1** than for **2**.

Tests of hydride cis migration on η^1(O) isomers do not allow us to identify any transition state: the η^1(O) coordination mode of the aldehyde does not activate the C═O double bond. We have also tested a pathway of direct hydrogenation of coordinated double bonds by dihydrogen: in this case also, no transition state has been found. These two tests show that both dihydrogen and the double bond have to be activated to lead to hydrogenation by this type of mechanism.

3.2. Reductive Elimination. In **6** and **7**, the hydride and the organic ligand are in trans positions and an isomerization is required before the reductive elimination can occur. The coordination of a phosphine prior to the reductive elimination is necessary to avoid the formation of 14-electron complexes, which are very unstable (moreover, the phosphines are in excess under the experimental conditions). Complexes **8** and **9** are obtained from **6** and **7**, respectively (see Figure 4), by the loss of the agostic interaction ($\Delta G^{\ddagger}$ = 33 and 35 kJ mol^{-1}, respectively) followed by coordination of a phosphine ligand (nonactivated to form **8** and $\Delta G^{\ddagger}$ = 23 kJ mol^{-1} to obtain **9**). In the case of **7**, the loss of the agostic interaction leads to a η^3(C,C,O) form which has to be isomerized to η^1(C) to accept

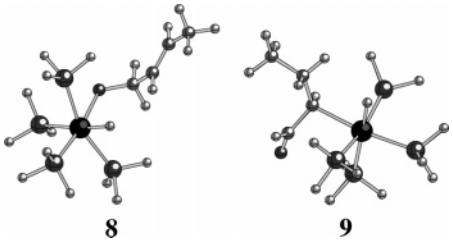

Figure 4. Precursor complexes for reductive elimination.

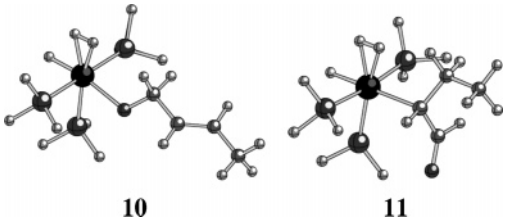

Figure 5. Product structures for dihydrogen coordination on **6** and **7**.

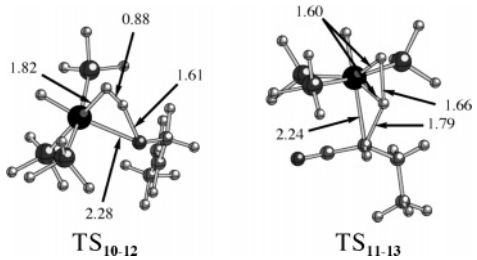

Figure 6. Transition states for σ-bond metathesis.

the coordination of the phosphine. This is why the coordination is activated to form **9** and not to form **8**.

Reductive eliminations from **8** and **9** require Gibbs free energies of 134 and 84 kJ mol^{-1}, respectively. Such barriers are very high, and another mechanism has to be found.

3.3. σ-Bond Metathesis. We noticed that it is necessary to activate both hydrogen and the double bond to perform the hydrogenation. As a result, starting from **6** and **7**, it is necessary to have coordination of dihydrogen on the Ru fragment to bring a new H. This reaction requires the agostic bond to be broken. Products structures **10** and **11** for the coordination of dihydrogen on **6** and **7**, respectively, are shown in Figure 5. The energetic data for these coordinations are reported in Table 1.

It can be noticed that there is no oxidative addition of dihydrogen on the Ru fragment, as it is a d^6 ML_5 fragment with π-acceptor ligands which stabilize and delocalize d orbitals and thus decrease the back-donation into the σ^*_{H-H} orbital.[21] The distance between the two hydrogens of the coordinated dihydrogen is 0.88 Å in **10** and 0.86 Å in **11**. The difference between the energy of reaction and the Gibbs free energy of reaction is mainly due to the loss of degrees of freedom (translation and rotation) of dihydrogen. It is in the range of those calculated for the usual reactions.[22]

With **10** and **11** as the starting points, four-center transition states for σ-bond metathesis have been found (see Figure 6). The products of the reaction, **12** and **13**, are represented in Figure 7, and the energetic data can be found in Table 1. The Gibbs free energy barrier for H−H/Ru-X σ-bond metathesis is higher in the case of X = O than in the case of X = C (25 kJ mol^{-1} vs 16 kJ mol^{-1}): the stabilization of the migrating hydride is better in TS_{11-13} than in TS_{10-12} (d_{Ru-H} = 1.60 Å in TS_{11-13} and d_{Ru-H} = 1.81 Å in TS_{10-12}). TS_{11-13} looks like a Ru(IV) trihydride, but it is really a transition state.

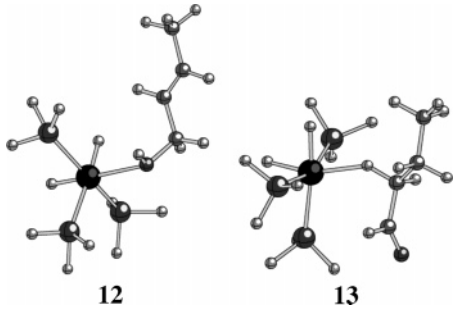

Figure 7. Products for σ-bond metathesis from **10** and **11**.

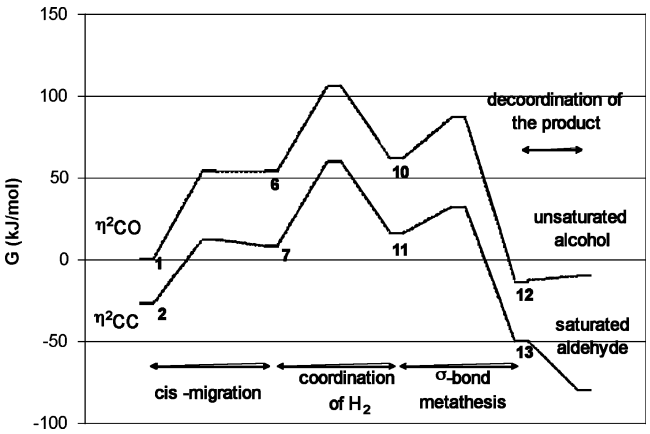

Figure 8. Gibbs free energy pathways for C=O and C=C hydrogenations.

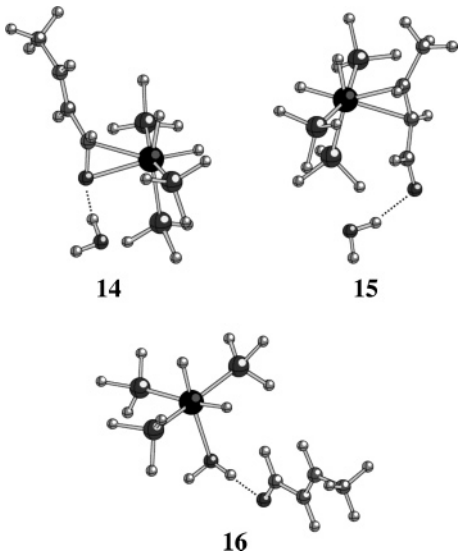

Figure 9. Coordinated water−crotonaldehyde adducts.

In the products, the organic molecule remains coordinated to the metallic fragment. For the alcohol obtained by hydrogenation of the C=O bond, a lone pair on the oxygen atom ensures coordination without rearrangement of the structure after the σ-bond metathesis (the bond strength between the alcohol and the Ru fragment in **12** is 66 kJ mol^{-1}). Because of the strength of the Ru−O bond the decoordination of the unsaturated alcohol from **12** is an endothermic process: ΔG = 3.9 kJ mol^{-1}.

In the case of the hydrogenation of the C=C bond, there is a bond in product **13** between the organic molecule and Ru via the hydrogen atom that comes from the σ-bond metathesis. It

(21) Jean, Y.; Eisenstein, O.; Volatron, F.; Maouche, B.; Sefta, F. *J. Am. Chem. Soc.* **1986**, *108*, 6587.

(22) Watson, L. A.; Eisenstein, O. *J. Chem. Educ.* **2002**, *79*, 1269.

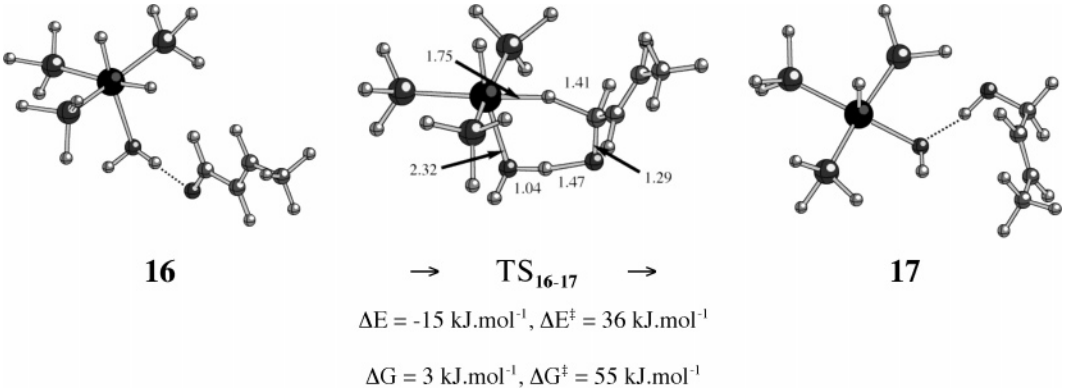

Figure 10. Simultaneous transfer of two hydrogen atoms on crotonaldehyde giving complex **17** from complex **16**.

costs 26 kJ mol^{-1} to break such a bond from an energetic point of view, but the decoordination of the saturated aldehyde from **13** is exothermic ($\Delta G = -30$ kJ mol^{-1}), as this bond strength cannot compensate the entropy gained in the decoordination process. As the decoordination is not activated, it will occur spontaneously.

The two decoordination processes lead to the dihydridotris(phosphine)ruthenium complex ($RuH_2(PH_3)_3$), which can be the starting point for another hydrogenation cycle.

The complete Gibbs free energy pathways for the C═O and C═C hydrogenations are reported in Figure 8. It is obvious from these pathways that a classical mechanism cannot explain the observed selectivity toward hydrogenation of C═O: the whole pathway for C═O hydrogenation is above the pathway for C═C hydrogenation, and all the barriers of C═O hydrogenation are higher than the barriers of C═C hydrogenation.

4. Water-Assisted Mechanism

In biphasic media, the ruthenium complex is in the aqueous phase due to sulfonated phosphines. The α,β-unsaturated aldehydes approaching the complex must go through the aqueous phase, or the catalysis may occur at the interface between organic solvent and water. As a result, the aldehyde is surrounded by water molecules and a hydrogen bond between water and the oxygen atom of the aldehyde is highly probable.

The hydrogen bond (see Figure 9) does not affect the relative stabilities of **1** and **2**, the free Gibbs energy between **14** and **15** being 26 kJ mol^{-1} in favor of **15**, as it is in favor of **2** compared to **1**. The two previous mechanisms are still correct in water.

The water−crotonaldehyde adduct can coordinate to the ruthenium complex via a lone pair of the water molecule. This leads to complex **16**, represented in Figure 9. **16** is less stable than **15**, $\Delta G_{\mathbf{16-15}} = 12$ kJ mol^{-1} ($\Delta E_{\mathbf{16-15}}$ is 34 kJ mol^{-1}), but more stable than **14**. While the model is improved by the insertion of the **15** and **16** structures in a polarizable dielectric continuum, the energy difference between **15** and **16** decreases to 29 kJ mol^{-1}. Hence, the solvent effect is small. The steric effect of more realistic phosphines has been modeled by the QM/MM approach, PPh_3 replacing PH_3 (with ONIOM as implemented in the Gaussian code). The energy difference between structures that correspond to **15** and **16** with PPh_3 is 23 kJ mol^{-1}. All the envisaged improvements reduce the energy difference between **15** and **16**, but the coordination of the C═C bond remains the most stable. In fact, the $\pi_{C=C}$ and the $\pi_{C=O}$ orbitals are mixed in the HOMO and the LUMO of crotonaldehyde.[4] Therefore, any perturbation, like the coordination of a water molecule, has an influence on the interaction of both C═O and C═C bonds with the metal. Only the coefficients differ in the mixing, which induces the small change in the energy difference.

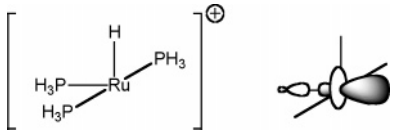

Figure 11. LUMO of $RuH(PH_3)_3^+$.

If Gibbs energy differences are considered, the situation in the case of PPh_3 ligands is totally inverted; the η^2(C,O)-coordinated **14** and, even more, the H_2O-coordinated complex **16** become more stable by far by 57 and 83 kJ mol^{-1}, respectively. However, the calculation of Gibbs free energy in the QM/MM calculations seems not to be relevant, as it depends on normal-mode calculations which are difficult to obtain with a good accuracy in the region between the QM and the MM parts. Thus, we prefer not taking into account the results obtained for ΔG with PPh_3 ligands.

Complex **16** can perform the hydrogenation of crotonaldehyde in a one-step reaction (see Figure 10). The water molecule induces an electrophilic assistance on the C═O function, which can then react with a hydride of the ruthenium complex. While the hydride is transferred to the carbon atom, the proton of the water molecule which interacts with the crotonaldehyde is transferred to the oxygen atom via a six-center transition state (see Figure 10), leading to the coordinated alcohol and an OH ligand.

Such a concerted transfer of two hydrogen atoms from the metal and one ligand (H_2O) looks like that observed for the hydrogenation of ketones by hydridodiamine ruthenium complexes, first observed by Noyori et al.[23] and confirmed by Morris et al.[24] In these cases, the hydrogen atoms come from Ru and the diamine. The same mechanism has also been found for a diamine Rh complex.[25] A similar mechanism involving H_2O as a hydrogen donor ligand has been observed in the hydrogenation reaction of CO_2.[26]

In complex **17**, the OH ligand has moved cis to the remaining hydride because of the trans influence of this hydride: the LUMO of the $RuH(PH_3)_3^+$ fragment is pointing trans to a phosphine (see Figure 11). This is related to the fact that it is energetically unfavorable for two strong σ-donor ligands to share

(23) Haack, K. J.; Hashiguchi, S.; Fujii, A.; Ikariya, T.; Noyori, R. *Angew. Chem., Int. Ed.* **1997**, *36*, 6.
(24) Abdur-Rashid, K.; Clapham, S. E.; Hadzovic, A.; Harvey, J. N. Lough, A. J.; Morris, R. H. *J. Am. Chem. Soc.* **2002**, *124*, 15104.
(25) (a) Guiral, V.; Delbecq, F.; Sautet, P. *Organometallics* **2001**, *20*, 2207. (b) Delbecq, F.; Guiral, V.; Sautet, P. *Eur. J. Org. Chem.* **2003**, 2092.
(26) Yin, C.; Xu, Z.; Yang, S. Y.; Man Ng, S.; Wong, K. Y.; Lin, Z.; Lau, C. P. *Organometallics* **2001**, *90*, 1216.

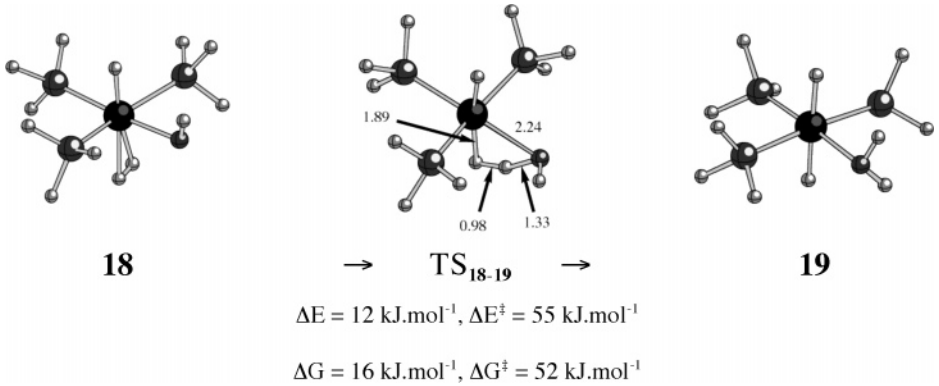

Figure 12. Regeneration of a trans dihydride ruthenium complex.

Scheme 4. Catalytic Cycle for the Water-Assisted Hydrogenation of the C═O Bond of Crotonaldehyde

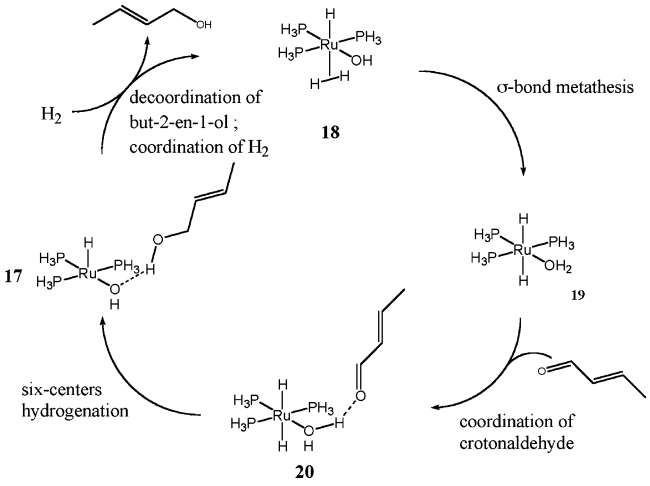

the same metal orbital.[27] This isomerization is simultaneous with the hydrogen transfer.

To regenerate a dihydride ruthenium complex, dihydrogen can coordinate on the remaining vacant position of **17**, trans to the hydride. This can occur after or before the release of the but-2-en-1-ol. The overall process is endoenergetic, $\Delta E = 43$ kJ mol^{-1} and $\Delta G = 50$ kJ mol^{-1}, and complex **18** is obtained (see Figure 12). In **18**, the H−H distance is only 0.79 Å and the Ru−H_2 distance is 1.86 Å, due to the trans influence of the hydride. Thus, dihydrogen is not strongly activated by the coordination on the metal: the activation barrier for the σ-bond metathesis **18** → **19** is higher than in the reaction **10** → **12**.

The dihydride that can be formed is not the cis isomer: the σ-bond metathesis described in Figure 12 leads to a trans dihydride and a coordinated water molecule. From complex **19**, hydrogenation of crotonaldehyde can restart via the catalytic cycle reported in Scheme 4. First crotonaldehyde coordinates via a water molecule to give **20** (equivalent to **16**). Then the hydrogenation through the six-center transition state, shown in Figure 13, gives **17** again. The energetic data for the whole catalytic cycle are reported in Figure 14. A comparison of TS_{16-17} and TS_{20-17} shows that the latter is earlier: C−H and O−H bonds are longer, and the C═O bond is less elongated. This is related to the smaller energy barrier.

Indeed, for the simultaneous transfer of hydrogen, $\Delta G^{\ddagger}$ is higher in the case of the cis dihydride **16**: 55 kJ mol^{-1} versus 15 kJ mol^{-1} starting from the trans dihydride **20**. The higher reactivity of the trans dihydride **20** can be understood as follows.

(27) Burdett, J. K.; Albright, T. A. *Inorg. Chem.* **1979**, *18*, 2112.

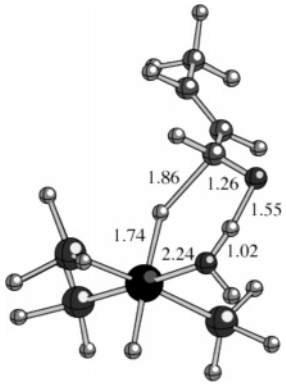

Figure 13. TS_{20-17}.

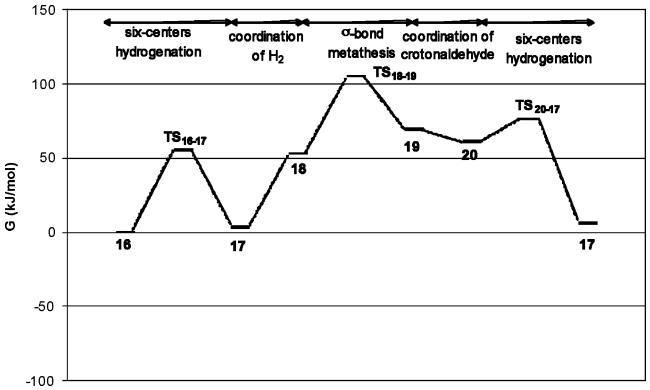

Figure 14. Gibbs free energy pathway for the water-assisted mechanism (for comparison, the same energy scale as in Figure 8 has been used).

First, **20** is less stable than **16**, due to the trans influence of the second hydride, which is stronger than the trans influence of a phosphine. When the Ru−H distance increases, the trans influence decreases. As a result, the energy difference between the two transition states TS_{16-17} and TS_{20-17} is not as large as it is for the two reactants: the activation barrier is lower in the case of the trans dihydride. Furthermore, the occupied molecular orbital localized on the migrating hydride in **16** is 1.3 eV lower than the occupied molecular orbital in **20** (it is the HOMO in **20** and HOMO-3 in **16**). Thus, the hydride in **20** is much more nucleophilic than the hydride in **16**. This is another way to express the hydride trans influence. This explains the higher reactivity of **20** toward hydride transfer. Furthermore, the interaction between the hydrogen atom of the water molecule and the oxygen atom of the aldehyde is stronger in **20** than in **16** (the overlap population is 16% higher in **20**). This is due to the stronger coordination of water trans to a phosphine (in **20**)

Scheme 5. Model Kinetic Scheme for Competitive Hydrogenation Cycles Giving SAL or UOL[a]

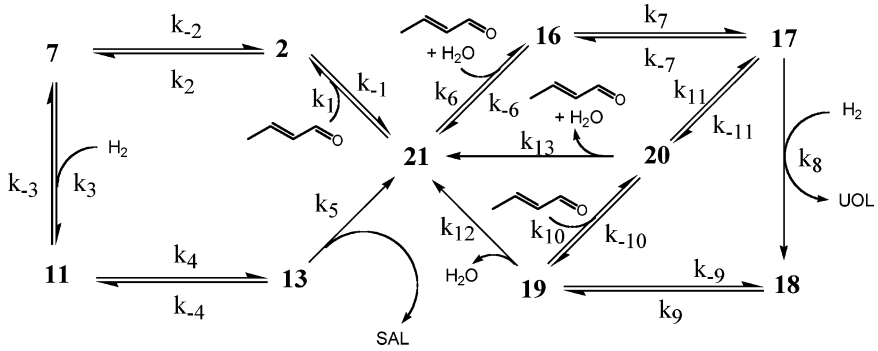

[a] **21** = *SPY*-5-*cis,mer*-[$RuH_2(PH_3)_3$].

Chart 1. Isomers of *SPY*-5-[$RuH_2(PH_3)_3$]

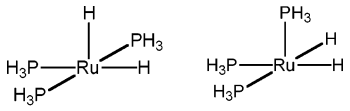

cis, mer *cis, fac*

as compared to that trans to a hydride (in **16**): the electron density is increased between Ru and O (32% higher in **20**), taking electrons from the O−H bond of the water molecule and weakening this bond. Hence, the hydrogen atom of the water molecule is more reactive in **20** than in **16**. The increase in reactivity of the two migrating hydrogens in **20** compared to those in **16** explains the smaller activation barrier for the six-center hydrogenation starting from **20**.

5. Kinetic Model for Selective Hydrogenation

From the two pathways for competitive hydrogenation of C═C by the classical mechanism and C═O by the water-assisted mechanism, it is not obvious that a selectivity toward C═O hydrogenation will be obtained, since the barriers are similar. We propose to test the competition between these two pathways by using the DFT values for activation barriers in the Eyring formalism, which gives the values of the kinetic constants:

$$k = \frac{k_B T}{h} e^{-\Delta G^{\ddagger}/RT}$$

For nonactivated exothermic elementary steps, we use $\Delta G^{\ddagger} = 0$ and for non activated endothermic elementary steps, we use $\Delta G^{\ddagger} = \Delta G$. As the reaction takes place in biphasic media, we suppose that the products—butanal (SAL) and but-2-en-1-ol (UOL)—move to the organic phase, while the complexes stay in the aqueous phase. As a result, the elementary steps which form SAL and UOL will not be reversible. The proposed kinetic scheme is reported in Scheme 5. The formation of *SPY*-5-*cis,mer*-[$RuH_2(PH_3)_3$] (**21**) starting from the identified precursor [$RuH_2(PH_3)_4$] has not been taken into account, since it affects the two competitive cycles in the same way: the decoordination of a phosphine must happen to coordinate the crotonaldehyde or the water molecule. The *mer* isomer (see Chart 1) has been preferred for this study, because of the trans effect of the hydride which induces the departure of a phosphine trans to the hydride in [$RuH_2(PH_3)_4$]. The energy difference between the *fac* and the *mer* isomers (see Chart 1) is 40 kJ mol^{-1} in favor of the *mer* isomer. The study of the interactions in these fragments has already been proposed.[4] Moreover, as mentioned above, the coordination of the aldehyde on the *mer* isomer gives **1** and **2**, which are more stable than the products of coordination on the *fac* isomer (**3**−**5**) for each coordination mode.

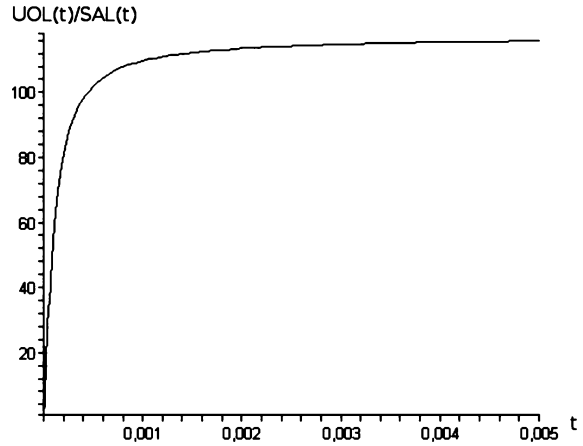

Figure 15. UOL/SAL ratio versus time (in s).

Under a continuous flow of crotonaldehyde that keeps the concentration of crotonaldehyde constant, this scheme leads to 12 coupled differential equations. The following values have been obtained for the kinetic constants: $k_1 = 6.2 \times 10^{12}$, $k_{-1} = 8.7 \times 10^8$, $k_2 = 6.4 \times 10^5$, $k_{-2} = 1.2 \times 10^{12}$, $k_3 = 4.7 \times 10^3$, $k_{-3} = 1.2 \times 10^5$, $k_4 = 9.7 \times 10^9$, $k_{-4} = 2.6 \times 10^{-2}$, $k_5 = 6.2 \times 10^{12}$, $k_6 = 6.2 \times 10^{12}$, $k_{-6} = 2.1 \times 10^{12}$, $k_7 = 1.4 \times 10^3$, $k_{-7} = 4.8 \times 10^3$, $k_8 = 1.1 \times 10^4$, $k_9 = 4.7 \times 10^3$, $k_{-9} = 3.0 \times 10^6$, $k_{10} = 6.2 \times 10^{12}$, $k_{-10} = 2.5 \times 10^{11}$, $k_{11} = 1.5 \times 10^{10}$, $k_{-11} = 3.3$, $k_{12} = 6.2 \times 10^{12}$, $k_{13} = 6.2 \times 10^{12}$. The total amount of ruthenium complex is 10^{-6} mol L^{-1} (the same order of magnitude as in reported experiments). We use [crotonaldehyde] $= 2 \times 10^{-4}$ mol L^{-1} and $[H_2] = 1$ mol L^{-1}; these two parameters affect the time scale of the kinetic model but do not affect the selectivity results. The analytical solution of the system of differential equations has been obtained with the Maple 9.5 software. The plot of the ratio [UOL]/[SAL] versus time is reported in Figure 15.

After a short induction period, products are formed with a constant rate. The ratio of concentration of products for C═O hydrogenation upon C═C hydrogenation is 120 after the induction period. This value is unchanged by the reactant concentration and is in agreement with the high selectivity (98%) experimentally observed. A test with an increase (10%) of the highest barrier in the cycle that forms UOL and a decrease of the highest barrier (10%) in the cycle that forms SAL does not affect the selectivity obtained by our model, even if this test clearly disfavors the formation of UOL. This shows that the model is not too sensitive to the errors from the DFT calculations.

To go further in the comprehension of the kinetics, we observed the concentrations of all the intermediates of the kinetic scheme after the induction period. It appears that **11** is in very low concentration compared with that of **7** and **19** is in very low concentration compared with that of **18**. This means that **7** → **11** and **18** → **19** are the determining steps of the two cycles. As they have the same rate constant ($k_9 = k_3$), the concentrations of **7** and **18** determine the rate of the cycle. During the stationary period, the concentration of **18** is 2 orders of magnitude higher than the concentration of **7**. Thus, the formation of UOL is faster than the formation of SAL.

During the induction period, we can see that the value of time needed for **18** to reach the stationary concentration of **7** is 1.5×10^{-5} s: after this time, the rate-determining step of the formation of UOL becomes faster than the rate-determining step of the formation of SAL and the selectivity increases beyond 50% to reach 98% when the stationary regime is obtained.

As k_7 is only 1.4×10^3, it is surprising that the step **16** → **17** is not a rate-determining step. In fact, **16** remains in high quantity (10 times as high as **18**) so that the product of the concentration and the rate constant is not as low as it is for the rate-determining steps that have been mentioned above.

Even though the activation barriers of the two cycles are quite similar and the stability of **16** is lower than that of **15**, the kinetic model proves a high selectivity toward C═O hydrogenation. Thus, the observed selectivity is a kinetic phenomenon.

6. Conclusion

As the two classical mechanisms cannot explain the selectivity of C═O hydrogenation in biphasic organic/aqueous media, the water-assisted mechanism allows us to justify the experimental observation. Although the η^2(C,C) coordination is thermodynamically preferred (−12 kJ mol^{-1}) compared to the coordination of a crotonaldehyde−water adduct by the water molecule, the kinetic model using Eyring theory that we can construct with DFT values for activation barriers reproduces the selectivity toward C═O hydrogenation. Kinetic considerations lead to the conclusion that, in biphasic organic/water media, the selectivity of C═O hydrogenation can be understood by the critical intervention of water in the mechanism.

Acknowledgment. We thank the Centre Informatique National de l'Enseignement Supérieur (CINES) at Montpellier and the Pôle Scientifique de Modélisation Numérique (PSMN) at ENS Lyon for CPU time.

OM050782A